文章编号:1006-9941(2022)07-0710-09

Catalytic Effects and Mechanisms of Metal-organic Complexes Mg(Salen) and Pb(Salen) on the Thermal Decomposition of HMX

MA Wen-zhe[1,2], YANG Yan-jing[3], ZHAO Feng-qi[3], LIU Xing-li[1], FU Dong-xiao[1], JIA Yu-xin[1], XU Kang-zhen[2]

(1. *Shaanxi Institute of Applied Physical Chemistry, Xi'an* 710061, *China*; 2. *School of Chemical Engineering, Northwest University, Xi'an* 710069, *China*; 3. *Xi'an Modern Chemistry Research Institute, Xi'an* 710065, *China*)

Abstract: The development of new combustion catalysts plays a key role in high performance propellants. Herein, the metal-organic complexes Mg(Salen) and Pb(Salen) were synthesized and characterized using X-ray diffraction, fourier transform infrared, and scanning electron microscope. Their catalytic effects on the thermal decomposition of 1,3,5,7-tetranitro-1,3,5,7-tetrazolidine (HMX) were further investigated by differential scanning calorimetry. The results indicate that the thermal decomposition of HMX is evidently enhanced by the introduction of Mg(Salen) and Pb(Salen). Compared with HMX, the decomposition peak temperatures of HMX/Mg(Salen) and HMX/Pb(Salen) dropped by 3.0 ℃ and 34.0 ℃, and theoretical apparent activation energies decreased by 7.7 kJ·mol^{-1} and 34.4 kJ·mol^{-1}, respectively. The catalytic decomposition mechanisms of Mg(Salen) and Pb(Salen) are also elucidated by exploring the decomposition kinetics and the reaction function models.

Key words: burning catalyst; HMX; salen; decomposition kinetics; solid propellant

CLC number: TJ55 **Document code**: A **DOI**: 10.11943/CJEM2022060

1 Introduction

The thermal decomposition characteristics of energetic components in solid rocket propellants have a profound effect on the combustion properties of the propellants[1-4]. HMX, a widely used energetic component, can improve the energetic performance of solid propellants[2]. However, large quantities of HMX in solid propellants lead to slow burning rates and high burning rate pressure indices, which are harmful to the performance reliability of solid motors[5-8]. Many studies have proven that one of the effective approaches to modulate the combustion performance of solid propellants is to add combustion catalysts[9-11]. Besides, the thermal decomposition properties of energetic compounds are closely related to their combustion properties in propellants[12-16]. According to the mechanism analysis, the reduction of the decomposition temperature of energetic materials is one of the most obvious characteristics of the combustion catalysis process of solid propellants[17-19]. Moreover, the development of compounds could adjust the thermal decomposition behavior of HMX and further optimize the combustion properties of solid propellants[2,9,20-23].

Compounds based on Schiff bases have various structures and possess many interesting properties. Specifically, they have been proved to have high catalytic activities in hydrogenation of cyclohexene reactions, carbene reactions, and nitrogen cycle reactions[24-26]. It is noticed that nitrogen cycle reactions are involved in the thermal decomposition of HMX and the combustion processes of propellants

Received Date: 2022-03-22; **Revised Date**: 2022-04-17

Published Online: 2022-06-01

Project Supported: National Natural Science Foundation of China (21673178)

Biography: MA Wen-zhe (1995-), male, assistant engineer, research field: solid propellant and pyrotechnic agent.
e-mail: mawz7344@163.com

Corresponding author: ZHAO Feng-qi (1963-), male, professor, research field: solid propellant and energetic materials.
e-mail: zhaofqi@163.com

引用本文:马文喆,杨燕京,赵凤起,等. 金属有机配合物Mg(Salen)和Pb(Salen)对HMX的催化分解作用和机理[J]. 含能材料,2022,30(7):710-718.
MA Wen-zhe, YANG Yan-jing, ZHAO Feng-qi, et al. Catalytic Effects and Mechanisms of Metal-organic Complexes Mg(Salen) and Pb(Salen) on the Thermal Decomposition of HMX[J]. *Chinese Journal of Energetic Materials (Hanneng Cailiao)*, 2022, 30(7):710-718.

containing HMX. Therefore, the metal Schiff base compounds are proposed to be potential catalysts for enhancing the decomposition and combustion of HMX[26]. N, N′-Bis (salicylidene) ethylenediamine, also called Salen ligand (Fig.1), is one of the widely used Schiff bases with an inner cavity between two salicylaldehyde moieties, which could accommodate suitable metal ions to form stable Salen metal complexes[28-29].

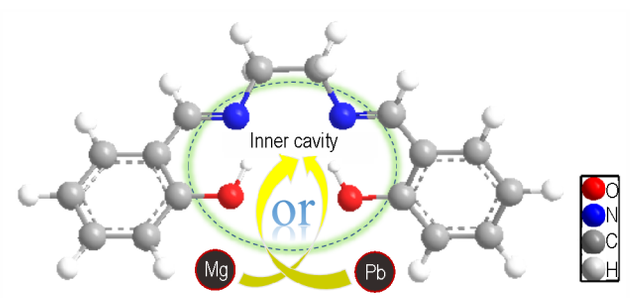

Fig.1 The structure of Salen ligand

Herein, N, N′-Bis (salicylidene) ethylenediamine-Mg and -Pd complexes were synthesized and presented as potential candidates for combustion catalysts of solid propellants, and their catalytic effects and mechanisms on the thermal decomposition of HMX were investigated.

2 Experimental

2.1 Materials

All chemicals used were commercially available. Salicylaldehyde (99.5%), ethylenediamine (99.9%), magnesium chloride (99.5%), lead (Ⅱ) nitrate (99.5%), and NaOH were purchased from Aladdin Inc. HMX was obtained from Xi'an Modern Chemistry Research Institute, and its purity was over 99%. Mg(Salen)/Pb(Salen) and HMX were mixed in a mass ratio of 1∶10 for the DSC tests.

2.2 Synthesis of Mg(Salen) and Pb(Salen)

N, *N*′-Bis (salicylidene) ethylenediamino (Salen) was prepared according to Reference [30]. Briefly, Salen and NaOH generate a sodium salt in ethanol solution. Then $MgCl_2·6H_2O$ or $Pb(NO_3)_2$ was added in the ethanol solution, and Mg (Salen) or Pb (Salen) complexes were obtained after stirring for 2 h. Mg (Salen): yield, 71.5%; elem. anal. (%), calcd for $C_{16}H_{14}N_2MgO_2$: C, 66.13; H, 4.86; N, 9.64; found: C, 66.53; H, 4.72; N, 9.19. Pb (Salen): yield, 63.2%; elem. anal. (%), calcd for $C_{16}H_{14}N_2PbO_2$: C, 40.72; H, 2.75; N, 5.89; found: C, 40.52; H, 4.79; N, 8.85.

2.3 Characterization

Elemental analysis (C, H, N) was performed on a Flash EA 1112 full-automatic trace element analyzer. X-ray diffraction (XRD) patterns were determined using a Rigaku Mini Flex 600 X-ray diffractometer with Cu Kα radiation (2θ from 5° to 60°). The vibrational characteristics of the chemical bonds were determined using a Bruker Tensor 27 Fourier transform infrared (FTIR) spectrometer. The morphologies of complexes were studied by scanning electron microscope (SEM). The differential scanning calorimetry (DSC) experiments were performed using a DSC200 F3 apparatus (NETZSCH, Germany) under nitrogen atmosphere at a flow rate of 80 mL·min^{-1}, and the heating rates were 5.0, 10.0, 15.0 ℃·min^{-1} and 20.0 ℃·min^{-1} from ambient temperature to 350 ℃, respectively. The TG/DTG experiments were performed using a SDT-Q600 apparatus (TA, USA) under nitrogen atmosphere at a flow rate of 100 mL·min^{-1}, and the heating rate was 10.0 ℃·min^{-1} from ambient temperature to 500 ℃.

3 Results and discussion

3.1 Structure and morphology

Salen is one of the most widely used organic Schiff base ligands. Fig.2a shows the XRD patterns of the as-prepared Salen and Salen complexes. It can be seen that the XRD pattern of Salen has low-density diffraction peaks with high intensity and narrow half-width, which is due to its great crystallinity and large size. Only a few diffraction peaks located at approximately 5.80°, 11.56°, 17.34°, 23.28° and 29.22° are present on the XRD pattern of Salen. However, there is no diffraction peaks of Salen in the XRD patterns of Mg(Salen) and Pb(Salen), indicating the absence of free Salen in complexes,

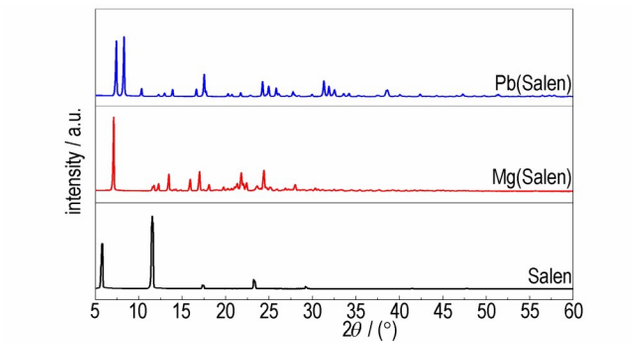

a. XRD

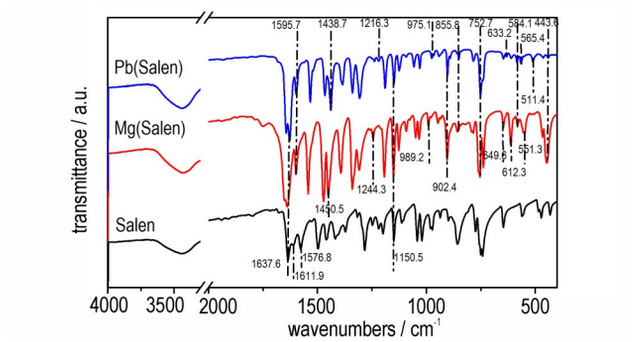

b. FTIR

Fig.2 XRD patterns and FTIR spectra of the Salen ligand, Mg(Salen) and Pb(Salen)

which confirms that these compounds are successfully synthesized. In addition, the high signal-to-noise ratio of the XRD patterns suggests the good crystallinity of both complexes.

The structural characteristics of Salen, Mg(Salen) and Pb(Salen) were further comfirmed by using FTIR spectroscopy. As shown in Fig. 2b, two stretching vibrational absorption bands of the bridging carbon-nitrogen double bond (1150.5 cm^{-1}) and the carbon-nitrogen single bond (1637.6 cm^{-1}) are detected on the spectra of Salen, Mg(Salen) and Pb(Salen), indicating that the bridging ethyl group does not participate in the coordination. Additionally, the two absorption peaks at 1576.8 cm^{-1} and 1611.9 cm^{-1} merge into one (1595.7 cm^{-1}) in Mg(Salen) and Pb(Salen), which can be attributed to the coordination of —OH with either the Mg ion or Pb ion. During the formation process of complexes, the bands at 1450.5, 1244.3, 989.2, 649.6, 612.3 cm^{-1} and 551.3 cm^{-1} indicate the presence of Mg—N coordination bonds in Mg(Salen). And the bands at 1438.7, 1216.3, 975.1, 633.2, 565.4 cm^{-1} and 511.4 cm^{-1} are attributed to the Pb-N bond in Pb(Salen). Besides, the absorption peaks appearing at 902.4, 752.7, 584.1 cm^{-1} and 443.6 cm^{-1} can be assigned to either the Mg—O or Pb—O coordination bonds, suggesting that the transition metal in the complexes is coordinated to the phenolic hydroxyl group.

As can be seen in Fig. 3, the Salen sample is composed of irregularly sheet particles with an average diameter of 0.3−1 μm, which are clearly agglomerated. However, many sheets with lengths of dozens of micrometers and widths of several micrometers are observed in the image of Mg(Salen), which reveals that it has a distinct 2D layered structure. The sheet surface of Mg(Salen) appears to be relatively smooth and the layered crystal structure is closely related to its morphology. However, the microscopic morphology of Pb(Salen) differs from that of Mg(Salen), showing numerous fibrous filaments. The filaments are between 100 nm and 500 nm in diameter, which provides the possibility of a high contact

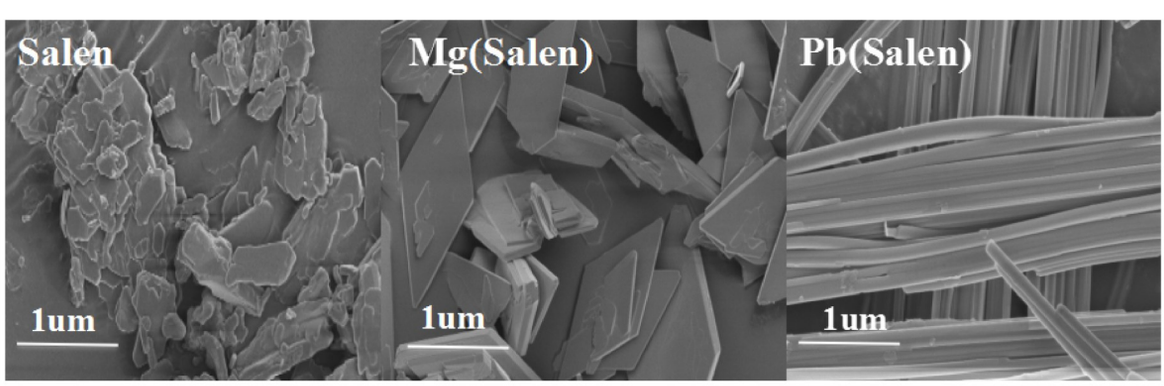

Fig.3 SEM images of the Salen ligand, Mg(Salen) and Pb(Salen)

activity of the catalyst due to its high surface area.

3.2 Thermal decomposition behavior

DSC curves of HMX/Mg(Salen) and HMX/Pb(Salen) are shown in Fig.4, and the HMX is measured for comparison. It can be seen that two peaks are detected for HMX from 100℃ to 350 ℃ at a heating rate of 10.0 ℃·min^{-1}, where an endothermic peak can be observed at 199 ℃ due to the transition of HMX from the low-temperature orthorhombic crystalline form to the high-temperature cubic form. HMX melts at 282.3 ℃ with the thermal decomposition. However, we can see a distinct change of the decomposition characteristics with the addition of Mg(Salen) or Pb(Salen). The exothermic decomposition peak temperature, T_p, of HMX/Mg(Salen) is 279.3 ℃, which is 3.0 ℃ lower than that of HMX. Surprisingly, the T_p of HMX/Pb(Salen) is reduced to 248.3 ℃, which presents a reduction of 34.0 ℃ compared to that of HMX. The results suggest that the decomposition of HMX is promoted by the addition of Mg(Salen) and Pb(Salen).

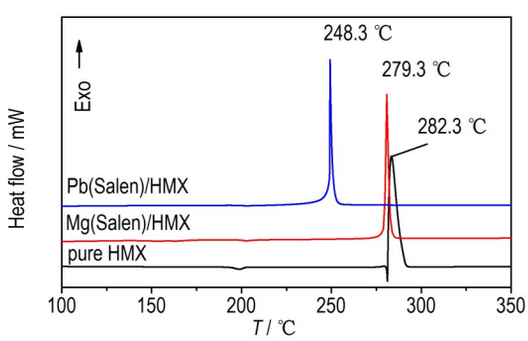

Fig.4 DSC curves of HMX, HMX/Mg(Salen) and HMX/Pb(Salen)

The TG/DTG curves of HMX, HMX/Mg(Salen), and HMX/Pb(Salen) were recorded at a heating rate of 10 ℃·min^{-1} and are shown in Fig.5. We can observe only one stage of mass loss for the three samples. The total mass loss of HMX is 97.4%, which is due to the fact that only the C residue remains in the decomposition products. However, the mass loss for HMX/Mg(Salen) and HMX/Pb(Salen) change from 97.4% to 69.1% and 76.3%, respectively, which may be due to the addition of the complexes that makes the decomposition products of HMX include some C residues and corresponding

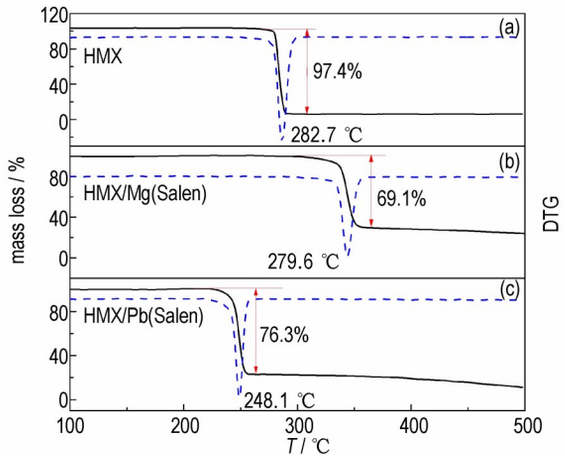

Fig.5 TG/DTG curves of HMX, HMX/Mg(Salen) and HMX/Pb(Salen)

metal oxides. The corresponding peak temperatures of DTG for HMX/Mg(Salen) and HMX/Pb(Salen) are advanced by 3.1 ℃ and 34.6 ℃, respectively, which agrees well with the DSC results.

The FTIR characteristic patterns of the gaseous pyrolysis products of HMX, HMX/Mg(Salen) and HMX/Pb(Salen) at the peak temperature are shown in Fig. 6. Although the positions of the absorption peaks of HMX/Mg(Salen) and HMX/Pb(Salen) are consistent with that of HMX, the absorption peak intensity of HMX/Mg(Salen) is lower. The phenomenon may be related to the sample amounts used in the test. Additionally, the strongest absorption double peaks at 2208 cm^{-1} and 2241 cm^{-1} can be attributed to N_2O (υ_{as}), the peaks at 1263 cm^{-1} and 1762 cm^{-1} are attributed to NO, and the peak around 2360 cm^{-1} belongs to CO_2. The sharp peak at 715 cm^{-1} may be formed by HCN, and the peaks at 1746 cm^{-1} and 2841 cm^{-1} can be assigned to HCHO. Meanwhile, the broad band near 2841 cm^{-1}

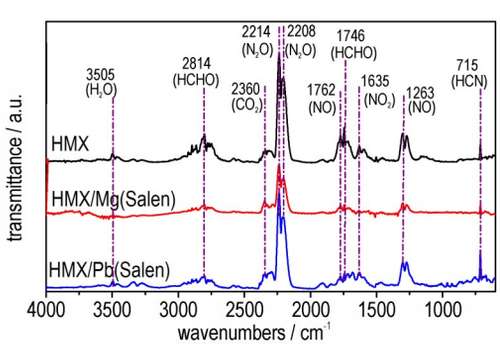

Fig.6 FTIR spectra of the gaseous products

is assigned to the rupture of the eight-membered heterocycle, indicating the cleavage of the C—N bond. The band around 3505 cm^{-1} can be attributed to the presence of H_2O, and the peaks at 1635 cm^{-1} is attributed to the generation of NO_2. Therefore, the pyrolysis gaseous products of HMX/Mg (Salen) and HMX/Pb(Salen) at the peak temperature are consistent with those of HMX, proving that the addition of the complexes does not change the nature of the decomposition products during the decomposition process. Based on this, the addition of Pb(Salen) or Mg (Salen) has an effect on the activation energy of HMX decomposition, but does not involve changes of the decomposition mechanism.

MS spectra show that all gaseous products are consistent during the decomposition of HMX and HMX/Salen (Fig. 7). The intense peaks at m/z=18 and m/z=44 are attributed to H_2O and CO_2 in HMX/Mg (Salen) and HMX/Pb (Salen). The existence of H_2O and CO_2 from the ambient environment is an external disruptive factor that must be taken into account throughout the test. Therefore, all gaseous products of HMX, HMX/Mg(Salen), and HMX/Pb (Salen) can be considered as consistent. The results indicate that the pyrolysis of HMX follows similar pathways under the three conditions.

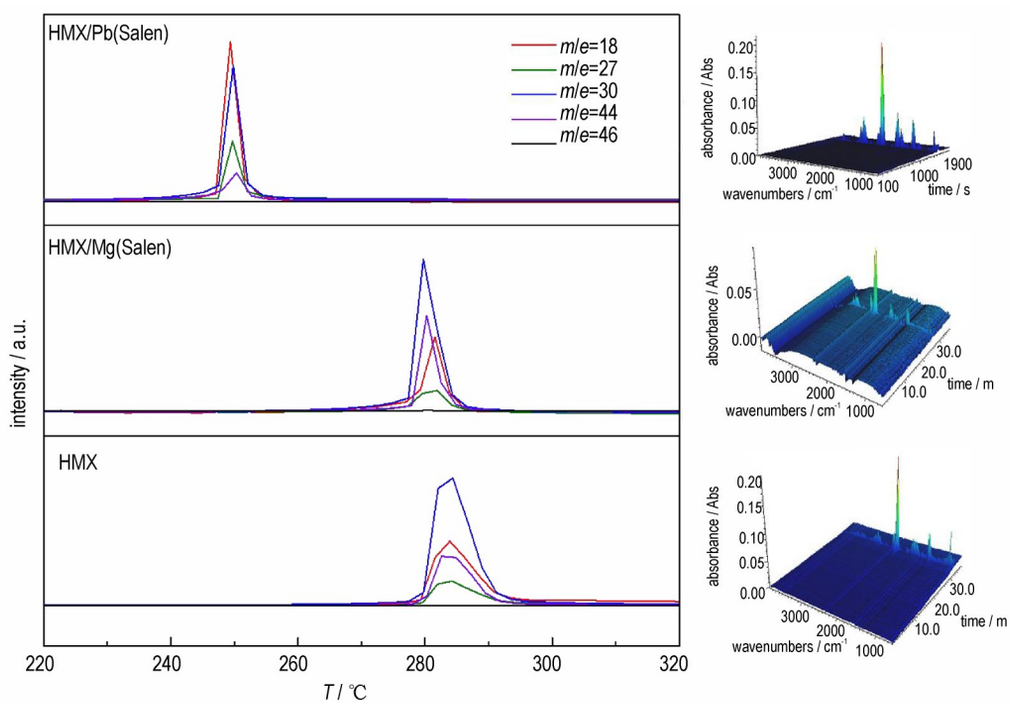

Fig.7 MS spectra of HMX, HMX/Mg(Salen) and HMX/Pb(Salen)

3.3 Apparent activation energy

To further investigate the catalytic properties of Mg(Salen) and Pb(Salen) for the thermal decomposition of HMX, the DSC curves of the samples were recorded at different heating rates, and the results are shown in Fig.8. The peak temperature (T_p), the apparent activation energy (E), and linear correlation coefficient (r) were calculated using Kissinger method and Ozawa method[7, 18] and are listed in Table 1.

From Table 1, we can see that the addition of

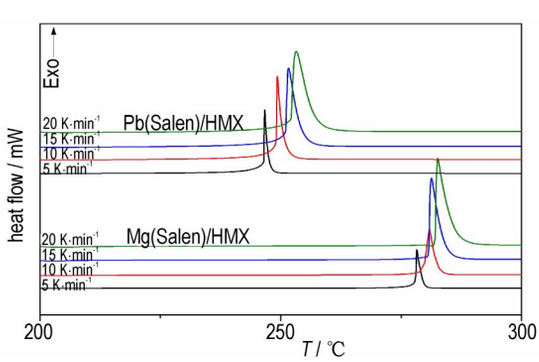

Fig.8 DSC curves of HMX/Mg(Salen) and HMX/Pb(Salen) at different heating rates

Table 1 Peak temperatures and kinetic parameters of the thermal decomposition of HMX, HMX/Mg(Salen) and HMX/Pb(Salen)

system	β/℃·min^{-1}	T_p/℃	E_k/kJ·mol^{-1}	r_k	E_o/kJ·mol^{-1}	r_o	$\bar{E}$
HMX	5	278.9	353.8	0.997	345.2	0.997	349.5
	10	283.4					
	15	286.1					
	20	288.9					
Mg(Salen)/HMX	5	273.1	345.9	0.985	337.7	0.9858	341.8
	10	279.3					
	15	281.3					
	20	282.6					
Pb(Salen)/HMX	5	244.1	318.4	0.998	311.7	0.9982	315.1
	10	248.3					
	15	251.6					
	20	253.6					

Note: β is the heating rate; T_p is the peak temperature; E_k and E_o are the apparent activation energies obtained by Kissinger method and Ozawa method, and $\bar{E}$ is the average value. r_k and r_o are the linear correlation coefficients obtained by Kissinger method and Ozawa method.

Mg(Salen) and Pb(Salen) decreases the apparent activation energy of the decomposition of HMX from 349.5 kJ·mol^{-1} to 341.8 kJ·mol^{-1} and 315.1 kJ·mol^{-1}, respectively. Meanwhile, Pb(Salen)/HMX has much lower apparent activation energy than Mg(Salen)/HMX, further indicating that Pb(Salen) is more effective than Mg(Salen) in catalyzing the thermal decomposition of HMX.

The values of E_a were obtained from DSC data at the different heating rates by Ozawa method, and the relationship between E_a and conversion (α) is shown in Fig.9. It can be seen that the activation energy slightly changes in the range of 0.35−0.95 (α), and this range was selected to calculate the non-isothermal reaction kinetic parameters and the most probable kinetic model functions.

Five integral methods (Agrawal, Satava-Sestak, MacCallum-Tanner, Universal integral, and General integral) were employed to calculate the kinetic equations. Forty-one kinetic model functions and the basic data were put into the integral and differential equations for the calculation[18,31-33]. The kinetic parameters and the probable kinetic model function were selected by the logical choice method and satisfying the ordinary range of the thermal decomposition kinetic parameters for energetic materials. These data together with their appropriate values of linear correlation coefficient (r) are presented in Table 2. The values of E_a and log$A$ that obtained from each single DSC curve are in good agreement with the values calculated by Kissinger method and Ozawa method. Therefore, it seems reasonable to conclude that the reaction mechanism for the intense exothermic decomposition process of HMX/Mg(Salen) and HMX/Pb(Salen) follows the Mampel power law equation $G(\alpha)=\alpha^{1/4}$. The $f(\alpha)$ variable in Eq. (1) can be substituted by $4\alpha^{3/4}$, while E_a can be replaced by 332.46 kJ·mol^{-1} or 316.34 kJ·mol^{-1}, and A by $10^{17.49}$ s^{-1} or $10^{18.7}$ s^{-1}.

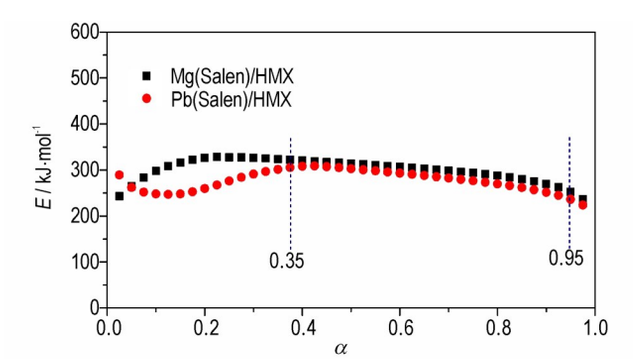

Fig.9 Curves of E_a versus α of HMX/Mg(Salen) and HMX/Pb(Salen) obtained by Ozawa method

$$\mathrm{d}\alpha/\mathrm{d}T = \frac{A}{\beta} f(\alpha) \mathrm{e}^{-E/RT} \quad (1)$$

where $f(\alpha)$ and $\mathrm{d}\alpha/\mathrm{d}T$ are the differential model function and the rate of conversion, respectively.

The kinetic equations of the exothermic decomposition reaction for HMX/Mg(Salen) and HMX/Pb(Salen) may be described as follows:

Table 2 Calculated values for the kinetic parameters of the decomposition reaction

method	β/℃·min^{-1}	HMX/Mg(Salen)			HMX/Pb(Salen)		
		E_a/kJ·mol^{-1}	log(A/s^{-1})	r	E_a/kJ·mol^{-1}	log(A/s^{-1})	r
Agrawal	5.0	337.9	20.34	0.9952	313.1	19.66	0.9862
	10.0	321.9	18.66	0.9816	315.6	16.86	0.9972
	15.0	333.8	17.30	0.9958	318.5	18.21	0.9887
	20.0	338.7	18.48	0.9868	319.0	15.23	0.9895
Satava-Sestak	5.0	330.0	19.77	0.9912	315.8	19.12	0.9873
	10.0	324.9	18.15	0.9826	309.8	16.40	0.9958
	15.0	331.1	17.06	0.9982	319.6	17.58	0.9891
	20.0	331.9	17.99	0.9876	314.2	17.83	0.9901
Mac Callum-Tanner	5.0	340.9	20.73	0.9892	315.3	19.97	0.9730
	10.0	324.8	19.04	0.9828	317.7	17.12	0.9858
	15.0	336.1	17.54	0.9862	316.5	17.79	0.9864
	20.0	331.7	18.87	0.9876	321.1	15.48	0.9902
The Universal integral	5.0	337.9	18.75	0.9855	312.5	18.06	0.9866
	10.0	322.0	17.11	0.9816	315.1	15.31	0.9956
	15.0	333.9	18.88	0.9956	318.1	16.57	0.9884
	20.0	338.9	16.95	0.9968	318.7	18.71	0.9895
The General integral	5.0	337.9	20.34	0.9916	313.1	19.66	0.9867
	10.0	321.9	18.66	0.9865	315.6	16.86	0.9865
	15.0	333.8	20.28	0.9956	318.5	18.21	0.9884
	20.0	338.8	18.48	0.9869	319.0	15.23	0.9895
Mean		332.5(E_{eo})	18.70		316.3(E_{eo})	17.49	
Ozawa		337.7(E_{po})		0.9858	311.7(E_{po})		0.9982
Kissinger		345.9(E_k)	11.13	0.9851	318.4(E_k)	20.24	0.9981
Mean(E_{eo}, E_{po}, E_k)		338.7			315.5		

Note: E with the subscripts eo and po are the apparent activation energies obtained from the onset temperature (T_e) and the peak temperature (T_p) by Ozawa method, respectively, and E with the subscript K is the apparent activation energy obtained from the peak temperature (T_p) by Kissinger method.

$$\mathrm{d}\alpha/\mathrm{d}T = 4\frac{10^{17.49}}{\beta}\alpha^{3/4}\exp(-3.99\times10^4/T) \quad (2)$$

$$\mathrm{d}\alpha/\mathrm{d}T = 4\frac{10^{18.7}}{\beta}\alpha^{3/4}\exp(-3.81\times10^4/T) \quad (3)$$

The thermal behavior of HMX was also analyzed using the same method. The results show that the reaction mechanism of the intense exothermic decomposition process can be described as $f(\alpha)=4(1-\alpha)^{3/4}$, $G(\alpha)=[1-(1-\alpha)]^{1/4}$, which differs from the decomposition mechanism function of HMX/Mg (Salen) and HMX/Pb (Salen). Thus, the addition of Mg (Salen) or Pb (Salen) obviously reduces the apparent activation energy and changes the kinetic model function of decomposition for HMX. Mg(Salen) and Pb (Salen) can accelerate the decomposition of HMX.

4 Conclusion

Mg (Salen) and Pb (Salen) were prepared and their structures were confirmed. Thermal analysis results show that these complexes can facilitate the decomposition of HMX. Mg(Salen) and Pb(Salen) can reduce the thermal decomposition peak temperature and apparent activation energy of HMX by 3 ℃ and 34 ℃, and 7.7 kJ·mol^{-1} and 34.4 kJ·mol^{-1}, respectively. The addition of Mg (Salen) or Pb (Salen) also changes the kinetic model function of the decomposition of HMX. The addition of Mg(Salen) and Pb(Salen) can significantly improve the thermal decomposition characteristics of HMX, which is beneficial for improving the combustion performance of HMX-containing propellants. They may be considered as combustion cat-

alysts for solid propellants.

References:

[1] YAN Qi-long, ZEMAN S, ZHANG Jian-guo, et al. Multi-step thermolysis mechanisms of azido-s-triazine derivatives and kinetic compensation effect for the rate-limiting processes[J]. *The Journal of Physical Chemistry*, 2015, 119(27): 14861−14872.

[2] YAN Qi-long, ZHAO Feng-qi, KUO K K, et al. Catalytic effects of nano additives on decomposition and combustion of RDX-, HMX-, and AP-based energetic compositions[J]. *Progress in Energy and Combustion Science*, 2016, 57:75−136.

[3] WU Qi, MA Qing, ZHANG Zhen-qi, et al. Combustion and catalytic performance of metal-free heat-resistant energetic polymeric materials[J]. *Chemical Engineering Journal*, 2020, 339: 125739−125771.

[4] XIAO Li-qun, FAN Xue-zhong, LI Ji-zhen, et al. Effect of Al content and particle size on the combustion of HMX-CMDB propellant[J]. *Combustion and Flame*, 2020, 214: 80−89.

[5] XIAO Li-qun, LI Ji-zhen, PEI Qing, et al. Combustion residues analysis of aluminized HMX-CMDB propellant[J]. *Chinese Journal of Explosives & Propellants*, 2021, 44(3): 361−366.
肖立群,李吉祯,裴 庆,等.含铝HMX-CMDB推进剂燃烧残渣特征分析[J].火炸药学报, 2021, 44(3): 361−366.

[6] MURAVYEV N, PIVKINA A, SCHOONMAN J, et al. Catalytic influence of nanosized titanium dioxide on the thermal decomposition and combustion of HMX[J]. *International Journal of Energetic Materials and Chemical Propulsion*, 2014, 13(3): 211−228.

[7] WEI Tao-tao, ZHANG Yu, XU Kang-zhen, et al. Catalytic action of nano Bi_2WO_6 on thermal decompositions of AP, RDX, HMX and combustion of NG/NC propellant[J]. *RSC Advances*, 2015, 5(86): 70323−70328.

[8] ZHAO Feng-qi, SHAN Wen-gang and LI Shang-wen. A review on silane coupling agents used in solid rocket motor charges and their cation mechanism [J]. *Chinese Journal of Energetic Materials*(*Hanneng Cailiao*), 1998, 6(1):37−42.
赵凤起,单文刚,李上文.有机硅烷偶联剂在固体火箭发动机装药中应用及其作用机理综述[J].含能材料, 1998, 6(1):37−42.

[9] YAN Qi-long. Discussion on the evaluation criteria of solid propellant combustion catalyst[J]. *Chinese Journal of Energetic Materials*(*Hanneng Cailiao*), 2019, 27(4): 266−269.
严启龙. 浅谈固体推进剂燃烧催化剂的评判标准[J]. 含能材料, 2019, 27(4): 266-269.

[10] LUO Yun-jun, XIA Min. Prospect of the functional addititives in energetic materials[J]. *Chinese Journal of Energetic Materials*(*Hanneng Cailiao*), 2021, 29(11): 1021−1024.
罗运军,夏敏.火炸药用功能材料发展趋势的思考[J].含能材料, 2021, 29(11):1021−1024.

[11] SARAH I, LOIR J G, ROBERT P L, et al. The effect of encapsulated nanosized catalysts on the combustion of composite solid propellants[J]. *Combustion and Flame*, 2015, 162(5): 1821−1828.

[12] MA Wen-zhe, ZHAO Feng-qi, YANG Yan-jing, et al. Effects of experimental conditions on catalytic efficiency of lead tannate on combustion of propellants[J]. *Chinese Journal of Energetic Materials*(*Hanneng Cailiao*), 2020, 28(2):170−176.
马文喆,赵凤起,杨燕京,等.制备条件对鞣酸铅催化燃烧活性的影响规律[J].含能材料, 2020, 28(2):170−176.

[13] ZHOU Shui-ping, WU Fang, TANG Gen, et al. Effects of 2CL-20/HMX cocrystals on the thermal decomposition behavior and combustion properties of polyether solid propellants[J]. *Energetic Materials Frontiers*, 2021, 2(2):96−104.

[14] WU Zong-kai, PEI Jiang-feng, SONG Xiu-duo, et al. Catalytic effects of nano-Fe_2O_3 and rGO-Fe_2O_3 on the thermal decomposition properties of CL-20/HMX cocrystal[J]. *New Journal of Chemistry*, 2020, 9(2):39−56

[15] MA Wen-zhe, ZHAO Feng-qi, LIU Xiao-lian, et al .Advancesin the researches on combustion catalysis of metal monocyclic aromatic complexes on DB and CMDB solid propellants[J]. *Chinese Journal of Explosives & Propellants*, 2019, 42(4): 319−327.
马文喆,赵凤起,刘晓莲,等.单环芳香族金属盐配合物对双基系固体推进剂的燃烧催化效果分析研究进展[J].火炸药学报, 2019, 42(4):319−327.

[16] YAN Qi-long, ZEMAN S, SELESOVSKY J, et al. Thermal behavior and decomposition kinetics of formex-bonded explosives containing different cyclic nitramines[J]. *Journal of Thermal Analysis and Calorimetry*, 2013, 111(2):1419−1430.

[17] YANG Yan-jing, BAI Yang, ZHAO Feng-qi, et al. Effects of metal organic framework Fe-BTC on the thermal decomposition of ammonium perchlorate[J]. *RSC Advance*. 2016, 6: 67308−67314.

[18] ZHAO Ning-ning, LI Jia-chen, GONG Hu-jun, et al. Effects of α-Fe_2O_3 nanoparticles on the thermal behavior andnon-isothermal decomposition kinetics of nitrocellulose[J]. *Journal of Analytical and Applied Pyrolysis*, 2016, 120(5):165−173.

[19] YANG Fan, DENG De-hui, PAN Xiu-lian, et al. Understanding nano effects in catalysis[J]. *National Science Review*, 2015, 2(2):183−201.

[20] AN Ting, CAO Hui-qun, ZHAO Feng-qi, et al. Preparation and characterization of Ag/CNTs nanocomposite and its effect on thermal decomposition of cyclotrimethylene trinitramine[J]. *Acta PhysicoChimica Sinica*, 2012, 28:2202−2208.

[21] WANG Ya-le, WEI Zhi-xian, KANG Li. Progress on combustion catalysts of solid propellant[J]. *Chinese Journal of Energetic Materials*(*Hanneng Cailiao*), 2015, 23(1):89−98.
王雅乐,卫芝贤,康丽.固体推进剂用燃烧催化剂的研究进展[J].含能材料, 2015, 23(1): 89−98.

[22] ZHANG Yu, WEI Tao-tao, XU Kang-zhen, et al. Catalytic decomposition action of hollow $CuFe_2O_4$ nanospheres on RDX and FOX-7[J]. *RSC Advance*, 2015, 5(92):75630−75635.

[23] ZHANG Hong-lei, JIAO Qing-jie, OU Ya-peng, et al. Pyrolysis pathway redirection of HNIW by nano-aluminum[J]. *Journal of Analytical and Applied Pyrolysis*, 2019, 11 (37) 293−298.

[24] XIA Qing-chun, LI Zi-jian, LIU Yan, et al. Synthesis, crystal structure and heterogeneous catalysis of a new chiral manganese coordination polymer based on the schiff-base ligand[J]. *Structural Chemistry*, 2018, 37(1):161−167.

[25] PANG Hai-xia, HUI Yong-hai, FAN Kui, et al. A catalysis study of mesoporous MCM-41 supported Schiff base and $CuSO_4 \cdot 5H_2O$ in a highly regioselective synthesis of 4-thiazolidinone derivatives from cyclocondensation of mercaptoacetic acid[J].*Chinese Chemical Letters*, 2016, 27(3):335−339.

[26] MA Wen-zhe, YANG Yan-jing, ZHAO Feng-qi, et al. Effects

of metal-organic complex Ni(Salen) on thermal decomposition of 1,1-diamino-2,2-dinitroethylene (FOX-7)[J]. *RSC Advance*, 2020, 10:1769-1775.

[27] CAO Peng, YANG Bin, WANG Jiang-ning, et al. Effect of organic bismuth-copper compound on combustion performances of DNTF/HMX-CMDB propellants[J]. *Chinese Journal of Explosives & Propellants*, 2016,39(4):82-86.
曹鹏,杨斌,王江宁,等.有机铋铜复盐对DNTF/HMX-CMDB推进剂燃烧性能的影响[J].火炸药学报,2016,39(4):82-86.

[28] CHOUDHARY A, KUMARI S, RAY S. Tuning of catalytic property controlled by the molecular dimension of palladium - Schiff Base complexes encapsulated in Zeolite Y[J]. *ACS Omega*, 2017, 2(10): 6636-6645.

[29] FEIZI H, SHIRI F, BAGHERI R, et al. The application of a nickel(Ⅱ) Schiff base complex for water oxidation: The importance of nanosized materials[J]. *Catalysis Science & Technology*, 2018, 8:3954-3968.

[30] WANKHEDE D S, HUSSAIN S, JADHAV N, et al. Synthesis and characterization of some biologically active mixed ligand complexes of transition metals such as Cr(Ⅲ),Mn(Ⅱ),Fe(Ⅲ), Co(Ⅱ), Ni(Ⅱ), Cu(Ⅱ) and Zn(Ⅱ)[J]. *Der Chemica Sinica*, 2013, 4(5):79-85.

[31] MA Hai-xia, YAN Biao, LI Zhao-na, et al. Preparation, non-isothermal decomposition kinetics, heat capacity and adiabatic time-to-explosion of NTO·DNAZ[J]. *Journal of Hazardous Materials*, 2009,169(3):1068-1073.

[32] MA Hai-xia, SONG Ji-rong, ZHAO Feng-qi, et al. Nonisothermal decomposition kinetics and computational studies on the properties of 2,4,6,8-tetranitro-2,4,6,8-tetraazabicyclo[3,3,1]onan-3, 7-dione (TNPDU)[J]. *The Journal of Physical Chemistry A*, 2017, 111(35):8642-8649.

[33] MA Hai-xia, YAN Biao, LI Zhao-na, et al. Synthesis, molecular structure, non-isothermal decomposition kinetics and adiabatic time to explosion of 3,3-dinitroazetidinium 3,5-dinitrosalicylate[J]. *Journal of Thermal Analysis and Calorimetry*, 2009,95: 437-444.

金属有机配合物Mg(Salen)和Pb(Salen)对HMX的催化分解作用和机理

马文喆[1,2],杨燕京[3],赵凤起[3],刘兴利[1],付东晓[1],贾玉馨[1],徐抗震[2]
(1.陕西应用物理化学研究所, 陕西 西安 710061; 2.西北大学化工学院, 陕西 西安 710069; 3.西安近代化学研究所, 陕西 西安 710065)

摘　要: 开发新型燃烧催化剂对提高推进剂燃烧性能至关重要。成功合成了2种席夫碱金属有机配合物Mg(Salen)和Pb(Salen),并采用X射线粉末衍射、红外光谱以及扫描电镜对其形貌与结构进行了表征。通过探索其热分解行为以及分解反应动力学函数模型考察了其对HMX热分解行为的影响与分解机理。结果表明,Mg(Salen)和Pb(Salen)的加入显著促进了HMX的热分解行为,但未改变其分解机理。相比于HMX,HMX/Mg(Salen)和HMX/Pb(Salen)的分解峰温分别降低了3.0 ℃和34.0 ℃,表观活化能分别降低了7.7 kJ·mol^{-1}和34.4 kJ·mol^{-1}。通过建立分解反应动力学函数模型,初步揭示了Mg(Salen)和Pb(Salen)对HMX的催化分解机理。

关键词: 燃烧催化剂;HMX;席夫碱;分解动力学;固体推进剂
中图分类号: TJ55　　**文献标志码:** A　　**DOI:**10.11943/CJEM2022060
(责编:王馨逸)